Process Biochemistry 45 (2010) 1800–1807

Contents lists available at ScienceDirect

Process Biochemistry

journal homepage: www.elsevier.com/locate/procbio

Control of the specific growth rate of *Bacillus subtilis* for the production of biosurfactant lipopeptides in bioreactors with foam overflow

S. Chenikher[a], J.S. Guez[b], F. Coutte[b], M. Pekpe[a], P. Jacques[b], J.P. Cassar[a,*]

[a] Laboratoire LAGIS, Polytech-Lille, Université Lille 1, Avenue Paul Langevin, Villeneuve d'Ascq, F-59655, France
[b] Laboratoire ProBioGEM, Polytech-Lille/IUT A, Université Lille 1, Avenue Paul Langevin, Villeneuve d'Ascq, F-59655, France

ARTICLE INFO

Article history:
Received 21 July 2009
Received in revised form 2 June 2010
Accepted 3 June 2010

Keywords:
Biotechnology
Fed-batch culture
Biosurfactant production
Open-loop control
Modeling
Extraction

ABSTRACT

This paper formulates a feeding law for a bioprocess dedicated to the production of an antibiotic surfactant using *Bacillus subtilis*. The specificity of the process relies on the use of the surface active property of the product to extract it by foaming. The control law is designed to maintain a constant specific biomass growth rate while taking into account the particularity of the process. This law can be regarded as a generalization of the conventional exponential feeding strategy and is generic enough to encompass the case of continuous processes with partial recycling. Conventional exponential feeding strategies indeed fail to account for the loss of biomass induced by the foaming. Previous experiments have provided a model of the process and values for its parameters. From this information, a feeding rate law was computed using the feeding strategy proposed in this paper and applied to an experimental culture. This experiment allows discussion of the modeling of the biomass extraction method used in this study. The results on the estimated specific growth rate highlight the complete agreement between the expected and experimental features. Further process optimization studies can now be performed on the basis of the constant specific biomass growth rate.

1. Introduction

The specific biomass growth rate is considered a key parameter in many bioprocess studies [1–4]. Indeed, it is correlated to other parameters such as production rates, which are essential for the design of industrial bioprocesses. These studies need to maintain a constant specific biomass growth rate during the experiment. Since the specific growth rate depends on the substrate concentration, this objective can generally be achieved by maintaining a constant feeding rate in continuous bioprocesses [5–7] or by providing an exponential feeding rate in fed-batch bioprocesses [1,3,8–10].

The originality of the mycosubtilin production bioprocess described and modeled by Guez et al. [11] is the use of the surface-active property of the product [12–14] to extract it continuously by foaming [15,16]. However, the foam also entraps some biomass quantity and consequently reduces the biomass quantity in the broth. This phenomenon makes it difficult to treat this bioprocess as a conventional fed-batch process. Model parameters were estimated in Ref. [11] from several exponential fed-batch experiments and were calculated for different target biomass growth rates without accounting for the foaming phenomenon. The partial loss of biomass was shown to induce increases in the biomass concentration and the specific biomass growth rate during the culturing step. To keep the specific growth rate constant, a new feeding law should consider the effect of the partial extraction of biomass introduced by foaming in future studies. In this way, the actual specific biomass growth rate can be correlated with the productivity or any other factor to be optimized.

With the very general biomass extraction model we have chosen, we can design a generic open-loop control law that is applicable to a wide variety of bioprocesses, such as those with partial recycling [17], fed-batch processes and our own specific process.

In the literature, various approaches for bioprocess control have been proposed [18–26]. Several control strategies developed in Ref. [27] leading to a closed-loop version of the conventional exponential feeding law for the regulation of specific biomass growth rate in fed-batch bioprocess could be applied to our control law. However, open-loop control was preferred given the lack of the available measurements of the state variables during the experiment and the difficulty of indirectly estimating the value of the specific biomass growth rate at any particular time using the measurements of biomass concentrations [28,29].

This open-loop feeding strategy was tested on an actual fed-batch culture of *Bacillus subtilis* involving the original foaming strategy. From the biological features of samples, as well as the measurements, the validity of the model used to compute the feed-

* Corresponding author. Tel.: +33 3 20 43 42 90; fax: +33 3 20 43 43 58.
E-mail address: jean-philippe.cassar@univ-lille1.fr (J.P. Cassar).

1359-5113/$ – see front matter © 2010 Elsevier Ltd. All rights reserved.
doi:10.1016/j.procbio.2010.06.001

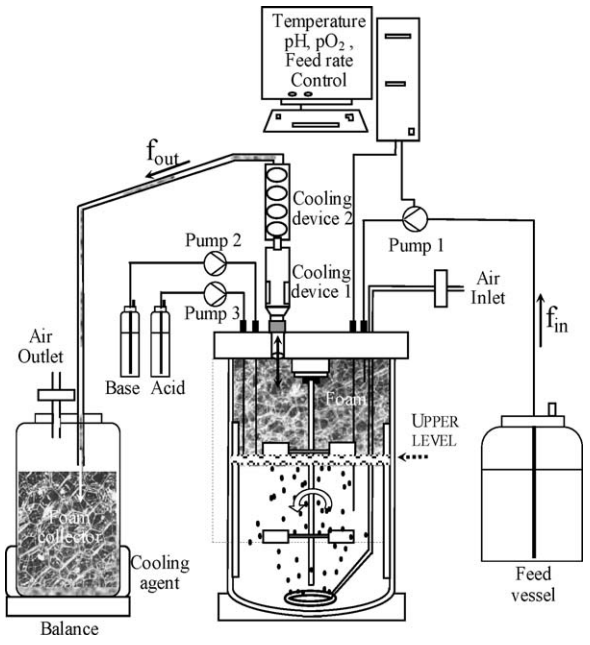

Fig. 1. Apparatus layout.

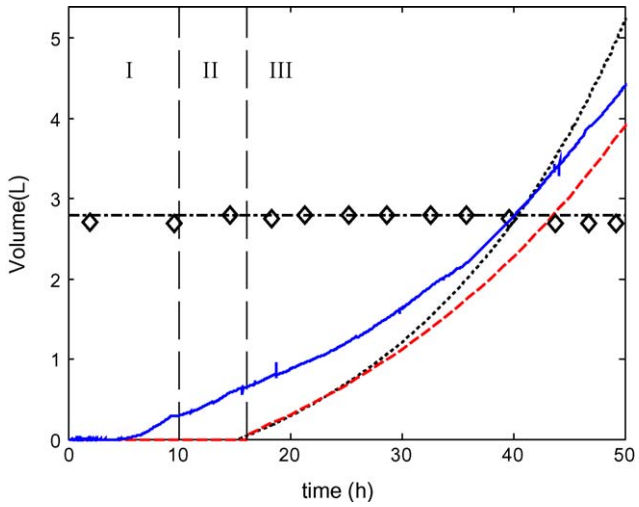

Fig. 2. Volumes in the bioreactor and in the collector: - - - reference volume in the bioreactor, (◊) measured volume V in the bioreactor, — measured volume in the collector, - - - - - - volume in the collector calculated with an exponential feeding profile, and – – – volume in the collector calculated with the proposed feeding profile.

ing strategy was checked, and the objective of achieving a constant specific biomass growth rate was verified.

This paper is organized as follows: Section 2 presents a brief description of the biosurfactant production process. The general dynamic model of the bioprocess for the three phases is given in Section 3. The design of the proposed new control law is highlighted in Section 4. Section 5 is devoted to the use of the available measurements to estimate the specific growth rate and biomass concentration in the effluent foam. The results obtained are presented in Section 6. Section 7 discusses the results with respect to the two following topics: the ability to obtain a constant specific growth rate and the validity of the model for biomass extraction by the foam. Finally, Section 8 outlines the conclusions of this work.

2. Biosurfactant production

2.1. Description of the process in bioreactor

This process was developed to extract lipopeptide biosurfactants like mycosubtilin and surfactin using their foaming properties. The description of this process design from a 5-L Bioflo 3000 bench-top fermenter (New Brunswick Scientific, Edison, MA, USA) is given in Fig. 1.

Instead of trying to avoid foaming, the foaming capacity of the broth was increased to collect the foam, which contains a high concentration of biosurfactant. For this purpose, the lower Rushton turbine was immersed in the broth to ensure the stirring of the broth and oxygen transfer. The upper impeller was fixed just above the initial height of the broth liquid. When a feeding flow caused the volume to increase, this impeller was progressively immersed in the liquid broth, favoring mixing at the gas–liquid interface. Clearly, the effect of this unusual impeller location was to drastically increase the foaming capacity at the gas–liquid interface. The foam was collected in a cooled foam collector.

The process was conducted in three main phases. In phase I, cells were grown for 10 h in a preliminary batch culture without feeding until the main carbon source was depleted. Early in this phase, foaming occurred and produced an overflow with a concomitant lowering of the liquid level. The foaming was due to the early production of mycosubtilin obtained with strain BBG100 and was caused by the replacement of the native *Pmyc* promoter with a constitutive one, *PrepU* [30].

The following two phases were aimed to ensure a constant specific growth rate under carbon-limiting conditions using appropriate feeding control laws. In phase II, because of the loss of broth in phase I, the level of the liquid remained below the level fixed by the upper propeller location; thus, there was no foaming caused by this upper propeller. The cells were grown in a fed-batch culture where the volume increased according to an exponential feeding law proposed by Yee and Blanch [1], whose expression is recalled in Section 4.1. The parameters of this feeding law were calculated from the initial biomass quantity, which was deduced from the analysis of the biomass concentration performed at the end of phase I. This phase ended when the liquid level reached the upper propeller; its duration was predicted from the feeding law and from the initial volume of the liquid.

In phase III, the liquid volume was kept constant because the feed flow was balanced by the increase of the foam overflow due to contact between the liquid and the upper propeller. In this phase, the new feeding control law developed in Section 4 was applied.

The evolutions with time of the volumes in the reactor and in the foam collector are given in Fig. 2 in Section 6.3 of the results with labels indicating the different phases of the process.

The temperature was regulated to 30 °C and the pH adjusted to 6.5 by adding 3 Moles L^{-1} solutions of KOH or H_2SO_4. The aeration rate was fixed at 0.75 L h^{-1}, and the dissolved oxygen concentration was maintained above 15% of the saturation concentration by maintaining the stirrer speed between 200 rpm and 500 rpm.

2.2. Bacterial strain and growth medium

The strain BBG100 used in this study is a mycosubtilin overproducer derivative obtained previously [30] from *B. subtilis* ATCC 6633 by the replacement of the native promoter of the mycosubtilin synthetase operon with a constitutive promoter originating from the replication gene (*repU*) of the *Staphylococcus aureus* plasmid pUB110. The pre-culture was inoculated in Erlenmeyer flasks containing a modified Landy medium described in Ref. [31] with 1 g L^{-1} of yeast extract added. The reactor containing the same medium was then inoculated with mid-logarithmic grown cells. The feeding medium was a double-concentrated Landy modified medium.

2.3. Analyses and measurements

2.3.1. Biosurfactant lipopeptides

Overflowed foam samples containing mycosubtilin were centrifuged at 10,000 g for 10 min. A volume of 1 mL of the supernatants was purified through C18 Maxi-Clean cartridges (Alltech, Deerfield, USA) as previously described by the authors [11]. The second derivative of the absorption spectrum between 200 nm and 400 nm (Diode Array PDA 996, Waters) was used to identify the eluted molecules (Millenium Software, Waters).

2.3.2. Biomass

The optical density at 600 nm was measured with a spectrophotometer (uV Mini 1 240, Shimadzu, Japan) whose precision is ±0.005 Abs (at 1 Abs) and ± 0.003 Abs (at 0.5 Abs). An optical density of 1.0 Abs corresponded to a biomass concentration of 0.33 g DW L^{-1}.

Samples were taken, and dilutions were performed using a P1000 Finnpipette (Thermo Fisher Scientific Inc., Waltham, MA, USA) whose precision is ±6 μL at 1000 μL and ±1 μL at 100 μL

2.3.3. Control and acquisitions

We used the software AFS Biocommand from New Brunswick Scientific for controlling the process and acquiring data. The weight of the foam collector was measured with a balance (DA 35 Ohaus, Pine Brook, NJ, USA) at a sampling period of 1 min.

3. Modeling

3.1. General model

The general dynamic model refers to the three phases of the bioprocess. The following model equations are deduced from volume or mass balances, in the bioreactor and in the foam collector (refer to the list of symbols for the meaning of the variables):

$$\frac{dVX}{dt} = \mu VX - X_{out} f_{out} \quad (1)$$

$$\frac{dVS}{dt} = -\frac{\mu}{Y_{X/S}} VX + S_{in} f_{in} \quad (2)$$

$$\frac{dV}{dt} = f_{in} - f_{out} \quad (3)$$

$$\frac{dV_{Col} X_{Col}}{dt} = X_{out} f_{out} \quad (4)$$

$$\frac{dV_{Col}}{dt} = f_{out} \quad (5)$$

Eq. (2) assumes that the foam does not remove any substrate, as the substrate concentration in the bioreactor is kept at a very low level.

The specific biomass growth rate should follow Monod's law:

$$\mu = \frac{\mu_{max} S}{K_s + S} \quad (6)$$

3.2. Theoretical models for phase I and phase II

The mass balance of biomass in both phases is deduced from the generic model, Eq. (1), by zeroing the output flow ($f_{out} = 0$):

$$\frac{dVX}{dt} = \mu VX \quad (7)$$

In the batch phase (phase I), there is no feeding flow, so: $f_{in} = 0$. Therefore, the model is reduced to Eq. (7), and the equation of substrate uptake is given by:

$$\frac{dVS}{dt} = -\frac{\mu}{Y_{X/S}} VX \quad (8)$$

From Eq. (3), the volume remains constant.

In the fed-batch phase (phase II), the dynamics of the substrate equation (2) does not change because the substrate concentration in the feeding flow is assumed to be constant. The volume balance in the bioreactor becomes:

$$\frac{dV}{dt} = f_{in} \quad (9)$$

A small foam overflow occurred in these phases but it was not taken into account in this theoretical model, which was used for simulation purposes.

3.3. Model for the phase with foam overflow (phase III)

In phase III, Eqs. (1)–(5) of the model are used with the addition of an equation to take account for biomass extraction by the foam.

$$X_{out} = \alpha X + \beta \quad (10)$$

This general model can thus deal with the three following scenarios:

X_{out} is proportional to X ($\alpha \leq 1$ and $\beta = 0$), corresponding to a partial recycling process,
X_{out} is equal to X ($\alpha = 1$ and $\beta = 0$), the bioprocess is considered continuous, without recycling,
$\alpha < 1$ and $\beta \neq 0$, corresponding to the foaming process and differs from existing bioprocess models.

4. Computation of the feeding flow control law

The new feeding flow control law $f_{in}(t)$ has to be designed to maintain the specific biomass growth rate constant. In Eq. (6), this variable only depends on substrate concentration, which has to also be kept constant. Therefore, the feeding control law required:

$$\frac{d\mu}{dt} = \frac{dS}{dt}\frac{d\mu}{dS} = \frac{dS}{dt}\frac{K_s \mu_{max}}{(K_s+S)^2} = 0 \Rightarrow \frac{dS}{dt} = 0 \quad (11)$$

4.1. Conventional exponential feeding flow control law

An exponential feeding profile was proposed by Yee and Blanch [1], for fed-batch processes (phase II).

From Eq. (2), the substrate dynamics are given by:

$$V\frac{dS}{dt} + S\frac{dV}{dt} = -\frac{\mu}{Y_{X/S}} VX + S_{in} f_{in}$$

Using Eq. (9), the following expression of the dynamics of the substrate concentration is derived:

$$\frac{dS}{dt} = -\frac{\mu}{Y_{X/S}} X + (S_{in} - S)\frac{f_{in}}{V} \quad (12)$$

When μ is constant, the differential equation (7) can be solved in VX and the solution is:

$$VX = V_0 X_0 \, e^{\mu t} \quad (13)$$

The feeding function can be calculated by substituting Eqs. (11) and (13) into Eq. (12):

$$f_{in}(t) = \frac{\mu}{Y_{X/S}(S_{in} - S_0)} VX = \frac{\mu}{Y_{X/S}(S_{in} - S_0)} V_0 X_0 \, e^{\mu t} \quad (14)$$

4.2. Control law for phase III

Using the exponential feeding equation (14) (Phase II), the specific growth rate was maintained at a constant value for the fed-batch culture without foam overflow. However, as soon as the foam starts to overflow the bioreactor, Eqs. (7) and (8), which are

based on the assumption that $f_{out} = 0$, are no longer valid. Indeed, we demonstrated in Ref. [11] that the exponential feeding law applied in the case of biomass extraction induces an increase of the specific biomass growth rate. Therefore, calculating a new feeding law is necessary to deal with the foam overflow and the substantial biomass extraction.

Eqs. (11) and (2) require that: $-(\mu/Y_{X/S})VX + S_{in}f_{in} = 0$, from which X can be deduced:

$$X = \frac{Y_{X/S}S_{in}}{\mu V}f_{in} \tag{15}$$

As already explained in the bioprocess description, the volume in the bioreactor remained constant during the whole of phase III. Substituting X from Eq. (15) into Eq. (1) with S, μ and V constant leads to:

$$V\frac{Y_{X/S}S_{in}}{\mu V}\frac{df_{in}}{dt} = \mu V\frac{Y_{X/S}S_{in}}{\mu V}f_{in} - X_{out}f_{in}$$

After simplification:

$$\frac{1}{\mu}\frac{df_{in}}{dt} = \left[1 - \frac{X_{out}}{Y_{X/S}S_{in}}\right]f_{in} \tag{16}$$

Substituting X_{out} from Eq. (10) into Eq. (16) gives:

$$\frac{1}{\mu}\frac{df_{in}}{dt} = -\frac{\alpha}{\mu V}f_{in}^2 + \left[1 - \frac{\beta}{Y_{X/S}S_{in}}\right]f_{in}$$

This equation is in the form of a Riccati equation:

$$\frac{1}{\mu}\frac{df_{in}}{dt} = af_{in}^2 + bf_{in} \quad \text{with} \quad a = -\frac{\alpha}{\mu V} \quad \text{and} \quad b = 1 - \frac{\beta}{Y_{X/S}S_{in}}$$

Its solution is given by:

$$f_{in}(t) = \frac{-b}{a - ((b + af_{in0})e^{-\mu bt}/f_{in0})} \tag{17}$$

With

$$f_{in(0)} = \frac{\mu}{Y_{X/S}S_{in}}V_0X_0$$

Feeding control laws for specific types of bioprocess can be developed from this general solution. The conventional exponential feeding profile is obtained by setting X_{out} to 0 and cancels out the second term of the RHS of Eq. (1), hence reverting to Eq. (7).

For continuous bioprocesses with recycling, where $X_{out} = \alpha X$, then $\beta = 0$ and $b = 1$, the feeding function is given by:

$$f_{in}(t) = \frac{-1}{a - ((1 + af_{in0})e^{-\mu t}/f_{in0})} \tag{18}$$

If the biomass concentration in the output flow is constant then $X_{out} = \beta$ ($\alpha = 0$), that leads to:

$$f_{in}(t) = f_{in0}e^{\mu bt} \tag{19}$$

4.3. Maintenance parameter effect

The maintenance parameter characterizes the phenomenon of substrate consumption by microorganisms for physiological reasons other than the growth. In the previous model (Sections 3.1 and 3.2), the consumption of the substrate was considered to be devoted entirely to biomass growth, and the maintenance parameter was supposed to be negligible. However, some authors have previously shown [11] that this parameter should not be neglected. Introducing the maintenance parameter into Eq. (2) leads to:

$$\frac{dS}{dt} = -\frac{\mu}{Y_{X/S}}X + (S_{in} - S)f_{in} - m_sX \tag{20}$$

The maintenance parameter does not change the parameter a, whereas the parameter b is written as:

$$b = 1 - \frac{\beta\left(1 - Y_{X/S}(m_s/\mu)\right)}{Y_{X/S}S_{in}}$$

5. Estimations from available measurements

We verified the validity of the proposed model for biomass concentration in the foam flow, as well as the efficiency of the feeding strategy to maintain the specific biomass growth rate constant, by estimating the evolution with time of these variables from the available measurements as described below.

5.1. Estimation of the biomass concentration in the foam X_{out}

The biomass concentration in the foam collector X_{Col} and the collected volume V_{Col} were measured and can be estimated from these measurements by Eqs. (4) and (5).

$$\hat{X}_{out} = \frac{d(V_{Col}X_{Col})/dt}{dV_{Col}/dt} \tag{21}$$

5.2. Estimation of the specific growth rate

Between two consecutive biomass measurements, only the mean value of the specific growth rate, which is considered constant, can be calculated.

For phase II, when neglecting the foam overflow from Eq. (7), the specific growth rate is given by:

$$\frac{dX}{X} = \mu\,dt \Rightarrow \ln X\Big|_{t_k}^{t_{k+1}} = \mu t\Big|_{t_k}^{t_{k+1}} \Rightarrow \ln X_{t_{k+1}} - \ln X_{t_k} = \mu(t_{k+1} - t_k)$$

$$\hat{\mu}_k = \frac{\ln\left(\frac{X_{t_{k+1}}}{X_{t_k}}\right)}{t_{k+1} - t_k} \tag{22}$$

In phase III, Eqs. (1) and (4) give:

$$\frac{dVX}{dt} = \mu VX - \frac{dV_{col}X_{col}}{dt}$$

The integration between t_k and t_{k+1} gives:

$$VX\Big|_{t_k}^{t_{k+1}} = \mu\int_{t_k}^{t_{k+1}} VX\,dt - V_{col}X_{col}\Big|_{t_k}^{t_{k+1}}$$

Therefore, the estimation of the mean value of μ in the interval $[t_k, t_{k+1}]$ is given by:

$$\hat{\mu}_k = \frac{[VX(t_{k+1}) - VX(t_k)] + [V_{col}X_{col}(t_{k+1}) - V_{col}X_{col}(t_k)]}{\int_{t_k}^{t_{k+1}} VX\,dt} \tag{23}$$

Because the quantity of biomass grows exponentially, the integration involve in the denominator of the RHS of Eq. (23) can be estimated by the trapeze method if the time interval remains short enough:

$$\int_{t_k}^{t_{k+1}} VX\,dt = \frac{1}{2}[VX(t_{k+1}) + VX(t_k)]$$

5.3. Uncertainties of the estimations

The uncertainties of the estimations, accounting for the accuracies of the measurement devices, are estimated by simulation using the Monte Carlo procedure performed for 1000 simulated samples. The uncertainties of measurements are supposed to be normally distributed with a standard deviation equal to the third of

Table 1
Parameter values of the bioprocess model.

Parameter	Values	Units
μ_{max}	0.35	h^{-1}
K_s	0.018	$g\,L^{-1}$
$Y_{X/S}$	0.22	$g\,g^{-1}$
m_s	0.07	$g\,g^{-1}\,h^{-1}$
α	0.001	–
β	2	$g\,L^{-1}$

the accuracy range. The choice of this distribution induces a probability of 0.01 of being out of the accuracy range. However, as the accuracy includes both deterministic and stochastic components, this choice overestimates the stochastic part of the uncertainties and thus the estimation of the intervals of confidence that are deduced from them.

To lower the effect of the derivation on the uncertainties, the derivate in Eq. (21) was computed from a polynomial approximation at order 2 of the evolution with time of the biomass quantity $V_{Col}X_{Col}$ in the collector. This approximation was obtained by a least squares fitting.

6. Results

6.1. Model parameters and experimental conditions

The specific bioprocess for producing mycosubtilin using *B. subtilis* and product recovery through foam is presented in more detail in Ref. [11]. In this paper, model parameters were estimated from a set of three experiments and further validated on six additional experiments.

These model parameters given in Table 1 were used to compute the feeding flow control laws and were also used to simulate the bioprocess behavior using models corresponding to the different phases.

The reference value of μ was fixed to $0.05\,h^{-1}$. This low μ value was the result of one limitation of the process, the maximal value of the feed flow, which was around $0.18\,L\,h^{-1}$. The limitation of the foaming flow and the maximum flow allowed by the feeding pump both contributed to this limitation of the feed flow.

The experiment was conducted at the ProBioGEM laboratory by managing the three phases (phases I, II and III) described in Sections 3.2 and 3.3. The initial conditions of theses phases are given in Table 2.

Phase I was initiated with an initial substrate concentration of $20\,g\,L^{-1}$. It lasted 10 h until the residual substrate concentration reached the value of $0.001\,g\,L^{-1}$.

For both phases II and III, the concentration of the substrate in the feeding flow was $S_{in} = 40\,g\,L^{-1}$. The conventional exponential feeding law for phase II (fed-batch) was calculated from the initial values of this phase so that the liquid level in the bioreactor reaches the propeller from the initial volume of 2.714 L. The equilibrium volume in the bioreactor that was obtained when the liquid reached the propeller was 2.8 L.

The feeding profile for phase III was calculated from Eq. (17) using the values of parameters and those of the initial conditions at the 16 h time point.

Table 2
Initial values of the variables X, S and V for the three phases (I, II and III).

Initials values of	V (L)	X ($g\,L^{-1}$)	S ($g\,L^{-1}$)
Phase I	3	0.08	20
Phase II	2.714	2.09	0.001
Phase III	2.8	2.7	0.001

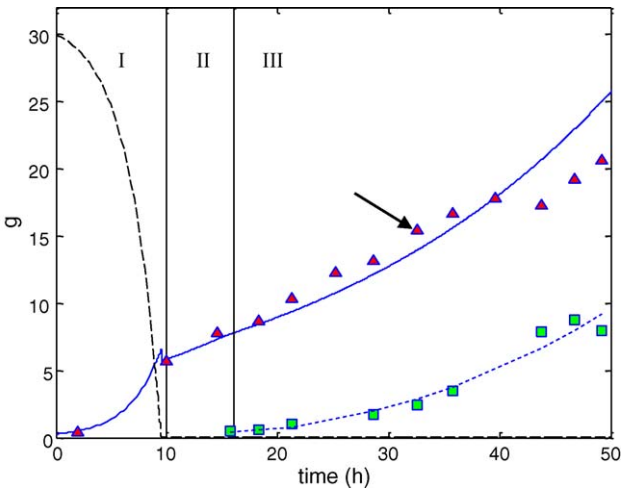

Fig. 3. Biomass and substrate quantities in the bioreactor and in the collector vessel: (▲) quantity of biomass in the bioreactor, (■) quantity of biomass in the collector vessel, — simulated biomass quantity in the bioreactor, - - - - - - polynomial approximation of the biomass quantity in the collector vessel, and – – – simulated quantity of substrate in the bioreactor.

The experiment was continued until the feeding flow pump maximal capacity around $0.18\,L\,h^{-1}$ was reached, *i.e.*, 40 h after the beginning of the feeding.

6.2. Volumes evolution with time

Fig. 2 provides the evolutions with time of the simulated and measured volumes both in the reactor and in the collector vessel.

The three phases that were explained in Section 2.1 are also presented here because they are closely related to the evolution with time of the volumes. In phases I and II, no foaming was expected from the simulation. In fact, the foam overflow already started in the middle of the batch phase and led to an increase in volume in the collector. This phenomenon also explains the quasi-constant gap between the expected and measured values of volume in the collector during phase III of the experiment.

The volume in the collector vessel was simulated using an exponential feeding law and is also given here for the purpose of comparison. The exponential feeding clearly led to a more important feeding flow and thus to a more important volume in the collector.

The foam overflow during phases I and II induced a loss of liquid volume in the bioreactor, which made it necessary to continue with phase II to recover the initial volume, while keeping constant the specific growth rate. In phase III, the broth volume in the bioreactor remained constant as the flow of foam balances the entire feeding flow.

6.3. Biomass quantities

The biomass quantities in the bioreactor and in the foam collector were calculated from volume and concentration measurements, which are given in Fig. 3. Intervals of confidence of 0.01 are depicted around the estimated values and are the result of the Monte Carlo procedure explained in Section 5.2.

The polynomial approximation of the order of 2 for the evolution with time of the biomass quantity in the collector that was introduced in Section 5.3 is also given in this figure. It provides the values of the biomass quantity in the bioreactor that was predicted by a dynamic simulation covering the three phases using the model of Eqs. (1)–(5) with the feeding flow calculated according to Eqs. (14) and (17).

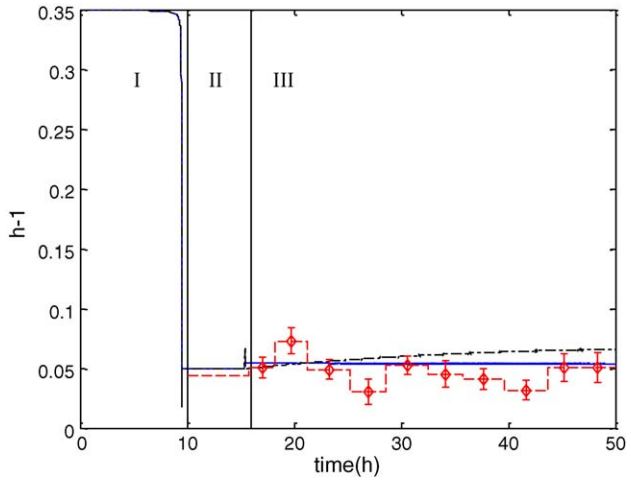

Fig. 4. Estimation of the specific biomass growth rate, – – – estimated value of μ interval of confidence of the estimated value of μ, - - - expected evolution with time of μ with an exponential feeding, and — simulated value of μ.

6.4. Estimation of the specific biomass growth rate

The objective of the control laws calculated from Eqs. (14) to (18) for phase II and phase III was to maintain the specific biomass growth rate at a constant value; Fig. 4 presents the estimations of this variable, which can be deduced from the measurements presented in the previous subsections using Eqs. (22) and (23).

Intervals of confidence at the 1% level are depicted around the estimated values and result from Monte Carlo simulation explained in Section 5.2.

The curves obtained by simulation for exponential feeding and the feeding calculated from Eq. (18) are also provided for the purpose of comparison.

6.5. Measurements and estimations of the biomass concentration in the foam

The measured values of the biomass concentration in the foam, X_{out}, were plotted against the measured concentration in the bioreactor in Fig. 5. Some additional data for the measurement of the biomass concentration in the foam were obtained from an independent experiment performed under the same conditions. Thus, a larger range of biomass concentrations in the reactor was covered.

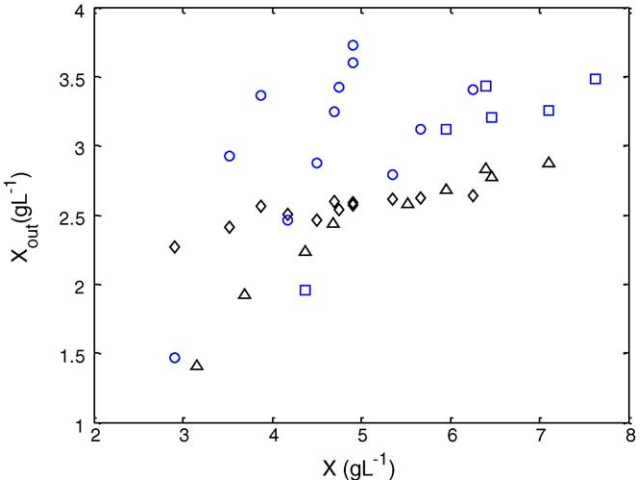

Fig. 5. Biomass concentration in the foam as a function of biomass concentration measured in the bioreactor, (□) X_{out} in the foam data from the experiment, (○) X_{out} in the foam from additional data, (△) estimated values of X_{out}, and (◊) estimated values of X_{out} from additional data.

Table 3
Mycosubtilin production and productivity during the experiment.

Time (h)	19.25	33.75	44.75	53.25
Mycosubtilin production (mg)	0	89.86	230.03	335.77
Mycosubtilin productivity (mg g^{-1} h^{-1})	0	0.46	0.71	0.61

The biomass concentration in the foam, X_{out}, was also estimated using Eq. (21). This estimation involved the time derivative of the quantity of biomass in the collector performed from the polynomial approximation of the time evolution with time of this variable, as depicted in Fig. 3. The slope of this curve provided the numerator of Eq. (21). The denominator was estimated from the slope of the time plot of the liquid volume in the collector in Fig. 2.

This information provided the basis for the discussion of the proposed linear model given in Eq. (10); the parameters α and β of this model obtained from previous experiments are given in Table 1.

6.6. Mycosubtilin production

Table 3 shows the quantities of mycosubtilin produced during the bioprocess. For experiments operated at a constant specific growth rate of 0.05 h^{-1}, the mycosubtilin productivity measured in our experiment at 0.71 mg g^{-1} h^{-1} agreed with the one obtained in a previous report [11], *i.e.*, 0.7 mg g^{-1} h^{-1}.

7. Discussion

7.1. Modeling of biomass extraction

In Fig. 5, the estimation of the biomass concentration, X_{out}, reached lower values than those measured in the foam. The latter can be explained by the dynamics of the foam in the collector vessel; the foam was driven into the collector with a delay and was slowly concentrated into a liquid. Therefore, the biomass concentration in the liquid did not take into account the total amount of biomass in the foam.

The difficulty in collecting a sufficient amount of foam to obtain analysis that was accurate enough led to a more important variability in the measurements of the biomass concentration in the foam.

In Fig. 5, the results of the experiment show that the relation between X_{out} and X did not exactly fit the model given by Eq. (10) and the parameters of Table 1. The minute value of α from the previous experiments implies that the biomass concentration in the foam was almost constant; it was equal to 2 g L^{-1}. This value was estimated for experiments conducted under different feeding conditions; few measurements were taken for each experiment. For $X = 0$, the biomass concentration in the foam must equal zero, and the proposed model did not take this constraint into account. The curvature of the experimental points scattering in the first experiment suggests that a non-linear model might better to fit these points, while satisfying this constraint.

However, for concentrations greater than 3 g L^{-1}; the points that were added from a second experiment do not confirm this hypothesis. This suggests that the structure of the proposed model can be validated with a greater value of the β parameter.

A computational prediction of the feeding control law using a value of $\beta = 3$. leads to a 17% increase of the feeding flow at the end of the experiment.

7.2. Results of the proposed control law

The main result of this paper is highlighted in Fig. 4, which plots the estimated specific biomass growth rate over time. The estimated values remained close to the expected value of 0.05 h^{-1}.

In phase III, the specific growth rate differed significantly from the target value during three separate periods. At the beginning of the application of the proposed feeding strategy, between times 15 h and 29 h, the specific growth rate was close to the reference value. From 18 h until 21 h 30 min, it increased significantly above the reference value and then ended below it from 25 h 25 min to 29 h. The mean value of the specific growth rate during the second period is close to the reference value. The third period from 35 h 75 min to 45 h 75 min, in which the specific growth rate was significantly lower than the target value, could reflect a substrate limitation problem. This effect was visible in Fig. 3, and the limitations presumed start is indicated by an arrow. The limitation in carbon substrate may be due to the open-loop control, which did not consider higher biomass concentrations than expected values. At the end of the fermentation, the value of μ was again very close to the reference value.

Interestingly, this result was obtained with open-loop control, demonstrating the relevance both of the model that was derived from previous experiments and of the calculated control law for the feeding flow. It is clear that a closed-loop scheme, based for example on predictive control, would limit all the observed fluctuations.

Introducing a maintenance parameter in the model led to a specific growth rate lower than the reference value. Indeed, in Section 4.3, parameter b increased when taking into account the maintenance phenomenon; thus the feeding was greater and led to a higher value of μ. The estimated values of μ were not influenced by the maintenance and were close to the reference. This indicates that this parameter could be eliminated as a contributing factor.

The comparison with the values of μ calculated for an exponential feeding shows that the proposed feeding strategy avoided an increase of the specific growth rate. Indeed, the equilibrium value of μ for an exponential feeding and a constant value of X_{out} have been demonstrated in Ref. [11] and it led to a value of 0.074 h^{-1} under the conditions of our experiment. However, under the new feeding law, this value cannot be reached because the feeding flow limitation only enables to run the experiment for 45 h instead of 50 h.

8. Conclusion

A new feeding control law has been proposed to keep the specific biomass growth rate constant even when biomass was partially extracted from the bioreactor. The new feeding control law differs fundamentally from the conventional exponential law. For instance, this feeding law was applied to keep the specific biomass growth rate at 0.05 h^{-1}. The estimations of the specific biomass growth rate based on the experimental measurements show the ability of the calculated control strategy to reach this objective, even in an open-loop configuration. Applying a closed-loop strategy, as a predictive control method based on the proposed feeding law, would improve these performances.

This study also provides better knowledge about biomass extraction using the foam overflow. For biomass concentrations in the bioreactor over 3 g L^{-1}, the relationship between the biomass concentration in the foam and in the bioreactor can be considered linear. The structure of the model proposed in a previous report is thus confirmed. Parameters of the biomass extraction model have been modified to express a constant biomass concentration in the foam at 3 g L^{-1}.

This new experiment confirms the correlation between the specific biomass growth rate and productivity of mycosubtilin obtained in previous works. Consequently, our results provide the basis for studies to maximize productivity of biosurfactants.

Acknowledgements

This work was supported by the Agence Nationale de la Recherche (ANR) and the European Funds for the Regional Development. The authors would like to thank Dr. William Everett for kindly reading the manuscript and Laurent Bonneau from Polytech-Lille for his technical assistance.

Appendix A. Nomenclature

V	volume of culture medium in the bioreactor (L)
V_{Col}	volume of culture medium in the collector (L)
V_0	volume of culture medium at the start of the feeding (L)
f_{in}	feeding rate (L h^{-1})
f_{out}	flow rate of overflow (L h^{-1})
X	biomass concentration in the bioreactor (g L^{-1})
X_{out}	biomass concentration in the foam (g L^{-1})
X_{Col}	biomass concentration in the collector (g L^{-1})
X_0	biomass concentration in the bioreactor at the feed beginning (g L^{-1})
S	substrate concentration in the bioreactor (g L^{-1})
S_{in}	substrate concentration in the feed (g L^{-1})
S_0	substrate concentrations in the bioreactor at the feed beginning (g L^{-1})
μ	specific growth rate (h^{-1})
μ_{max}	maximum specific growth rate (h^{-1})
K_s	saturation constant (g L^{-1})
$Y_{X/S}$	actual growth yield on substrate (g g^{-1})
m_s	maintenance coefficient (g g^{-1} h^{-1})
α	proportional coefficient of the linear model of biomass concentration in the foam
β	constant coefficient of the linear model of biomass concentration in the foam (g L^{-1})

References

[1] Yee L, Blanch HW. Recombinant protein expression in high cell density fed-batch cultures of *Escherichia coli*. Nat Biotechnol 1992;10(12):1550–6.
[2] Loloei AZ, Daneshp N, Motlagh MRJ, Vali AR. Growth rate control in biotechnological fed-batch process using dynamic matrix control. In: SICE-ICASE International Joint Conference. 2006. p. 3696–701.
[3] Martiĩnez A, Ramiĩrez OT, Valle F. Effect of growth rate on the production of β-galactosidase from *Escherichia coli* in *Bacillus subtilis* using glucose-limited exponentially fedbatch cultures. Enzyme Microb Tech 1998;22(6):520–6.
[4] Bastin G, Dochain D. On-line Estimation and Adaptive Control of Bioreactors. Amsterdam: Elsevier Science; 1990.
[5] Dauner M, Storni T, Sauer U. *Bacillus subtilis* metabolism and energetic in carbon-limited and excess-carbon chemostat culture. J Bacteriol 2001;183(24):7308–17.
[6] Vierheller C, Goel A, Peterson M, Domach MM, Ataai MM. Sustained and constitutive high levels of protein production in continuous culture of *Bacillus subtilis*. Biotechnol Bioeng 1995;47:520–4.
[7] Zamboni N, Fisher E, Muffler A, Wyss M, Hohmann HP, Sauer U. Transient expression and flux changes during a shift from high to low riboflavin production in continuous cultures of *Bacillus subtilis*. Biotechnol Bioeng 2005;89(2):219–32.
[8] Lee J, Parulekar SJ. Enhanced production of α-amylase in fed-batch cultures of *Bacillus subtilis* TN 106[pAT5]. Biotechnol Bioeng 1993;42:1142–50.
[9] Picó-Marco E, Navarro JL, Bruno-Barcena JM. A closed loop exponential feeding law: Invariance and global stability analysis. J Process Control 2006;16(4):395–402.
[10] Picó-Marco E, Picó J. Partial stability for specific growth rate control in biotechnological fed-batch processes. J Process Control 2003;1:724–8.
[11] Guez JS, Chenikher S, Cassar JP, Jacques P. Setting up and modelling of overflow fed-batch cultures of *Bacillus subtilis* for the production and continuous removal of lipopeptides. J Biotechnol 2007;131(1):67–75.
[12] Maget-Dana R, Thimon L, Peypoux F, Ptak M. Surfactin/iturin A interactions may explain the synergistic effect of surfactin on the biological properties of iturin A. Biochimie 1992;74:1047–51.
[13] Razafindralambo H, Paquot M, Baniel A, Popineau Y, Hbid C, Jacques P, Thonart P. Foaming properties of surfactin, a lipopeptide biosurfactant from *Bacillus subtilis*. J Am Oil Chem Soc 1996;73(1):149–51.

[14] Razafindralambo H, Popineau Y, Deleu M, Hbid C, Jacques P, Thonart P, Paquot M. Foaming properties of lipopeptides produced by *Bacillus subtilis*: effect of lipid and peptide structural attributes. J Agric Food Chem 1998;46:911–6.
[15] Cooper DG, Macdonald CR, Duff SJ, Kosaric N. Enhanced production of surfactin from *Bacillus subtilis* by continuous product removal and metal cation additions. Appl Environ Microbiol 1981;42:408–12.
[16] Davis DA, Lynch HC, Varley J. The application of foaming for the recovery of surfactin from *B. subtilis* ATCC 21332 cultures. Enzyme Microb Technol 2001;28:346–54.
[17] McIntyre JJ, Bunch AW, Bull AT. Vancomycin production is enhanced in chemostat culture with biomass-recycle. Biotechnol Bioeng 1999;62:576–82.
[18] Harmand J, Rapaport A, Dochain D, Lobry C. Microbial ecology and bioprocess control: opportunities and challenges. J Process Control 2008;18(9):865–75.
[19] Dochain D. State observation and adaptive linearizing control for distributed parameter (bio)chemical reactors. Int J Adapt Control Signal Process 2001;15:633–53.
[20] Huang B. Bayesian methods for control loop monitoring and diagnosis. J Process Control 2008;18(9):829–38.
[21] Dowd JE, Ezra KE, Kwok, Piret JM. Predictive modeling and loose-loop control for perfusion bioreactors. Biochem Eng J 2001;9:1–9.
[22] Lee J, Lee SY, Park S, Middelberg APJ. Control of fed-batch fermentations. Biotechnol Adv 1999;17:29–48.
[23] Gadkar KG, Doyle FJ, Crowley TJ, Varner JD. Cybernetic model predictive control of a continuous bioreactor with cell recycle. Biotechnol Prog 2003;19: 1487–97.
[24] Magyar A, Szederkényi G, Hangos KM. Globally stabilizing feedback control of process systems in generalized Lotka–Volterra form. J Process Control 2008;18:80–91.
[25] Morari M, Lee HJ. Model predictive control: past, present and future. Comput Chem Eng 1999;23:667–82.
[26] Zhu GY, Zamamiri A, Henson MA, HjortsØ MA. Model predictive control of continuous yeast bioreactors using cell population balance models. Chem Eng Sci 2000;55:6155–67.
[27] De Battista H, Picó J, Picó-Marco E. Globally stabilizing control of fed-batch processes with haldane kinetics using growth rate estimation feedback. J Process Control 2006;16(8):865–75.
[28] Jenzsch M, Simutis R, Eisbrenner G, Stückrath I, Lübbert A. Estimation of biomass concentrations in fermentation processes for recombinant protein production. Bioprocess Biosyst Eng 2006;29(1):19–27.
[29] Jenzsch M, Simutis R, Luebbert A. Generic model control of the specific growth rate in recombinant *Escherichia coli* cultivations. J Biotechnol 2006;122(4):483–93.
[30] Leclère V, Béchet M, Adam A, Guez JS, Wathelet B, Ongena M, Thonart P, Gancel F, Chollet-Imbert M, Jacques P. Characterization of a constitutive mycosubtilin overproducing *Bacillus subtilis* strain and its antagonistic activity. Appl Environ Microbiol 2005;71(8):4577–84.
[31] Guez JS, Muller CH, Danzé PM, Büchs J, Jacques P. Respiration activity monitoring system (RAMOS), an efficient tool to study the influence of the oxygen transfer rate on the synthesis of lipopeptide by *Bacillus subtilis* ATCC6633. J Biotechnol 2008;134(1–2):121–6.